Molecular interactions between *Tbx3* and *Bmp4* and a model for dorsoventral positioning of mammary gland development

Kyoung-Won Cho*, Jae-Young Kim*, Soo-Jin Song*, Elizabeth Farrell†, Maxwell C. Eblaghie†‡§, Hee-Jin Kim*, Cheryll Tickle†, and Han-Sung Jung*¶

*Division in Anatomy and Developmental Biology, Department of Oral Biology, Research Center for Orofacial Hard Tissue Regeneration, Brain Korea21 Project, Oral Science Research Center, College of Dentistry, Yonsei Center of Biotechnology, Yonsei University, Seoul 120-752, Korea; †Division of Cell and Developmental Biology, Faculty of Life Science, The Wellcome Trust Biocentre, University of Dundee, Dundee DD1 4HN, Scotland, United Kingdom; and Departments of ‡Cell Biology and §Ophthalmology, Duke University Medical Center, Durham, NC 27710

Edited by Kathryn V. Anderson, Sloan–Kettering Institute, New York, NY, and approved August 16, 2006 (received for review June 5, 2006)

The formation of the dorsoventral (DV) boundary is central to establishing the body plan in embryonic development. Although there is some information about how limbs are positioned along the DV axis and how DV skin color pattern is determined, the way in which mammary glands are positioned is unknown. Here we focus on *Bmp4* and *Tbx3*, a gene associated with ulnar-mammary syndrome, and compare their expression along the DV axis in relation to mammary gland initiation in mouse embryos. *Tbx3* is expressed in the mammary gland-forming region with *Tbx15*, a gene involved in a DV coat color being expressed more dorsally and *Bmp4* being expressed more ventrally. When *Tbx3* was overexpressed, formation of mammary gland epithelium was extended along the DV axis. In contrast, overexpression of *Bmp4* inhibited both *Tbx3* and *Tbx15* expression. In addition, when BMP signaling was inhibited by NOGGIN, *Lef1* expression was lost. Thus, we propose that mutual interactions between *Bmp4* and *Tbx3* determine the presumptive DV boundary and formation of mammary glands in early mouse embryogenesis. 1,19-Dioctadecyl-3,3,39,39-tetramethyl indocarbocyanine perchloride labeling experiments showed that cells associated with mammary glands originate more dorsally and then move ventrally. This finding, together with previous findings, suggests that the same DV boundary may not only position limbs and determine coat color but also position mammary glands. Furthermore, *Bmp* signaling appears to be a fundamental feature of DV patterning.

dorsoventral patterning | ulnar-mammary syndrome

A key event in vertebrate embryogenesis is establishment of the main body axes, anteroposterior (head to tail) and dorsoventral (DV; back to front), and specifying cell position along them to give the body plan. One mechanism for specifying cell position is through the response to gradients of various extracellular signaling molecules (1). Positional information is then encoded by expression of transcription factors that control subsequent development of that region of the embryo, and this ensures that organs are initiated in the correct locations. Striking examples of organs that develop at a particular DV level are the mammary glands (2). These arise along mammary lines that form at the boundary between anterior and lateral cutaneous nerve branches (3, 4) and run in an anteroposterior direction between forelimb and hindlimb (5, 6). These mammary lines are morphologically evident in the flank (interlimb region) of rabbit embryos and are marked by expression of several different genes, including *Lef1* and *Wnt10b*, in mouse embryos (7). Here we examine mammary gland initiation and positioning with respect to DV body patterning in mouse embryos and examine the roles of Bmp signaling and genes that encode Tbx transcription factors.

Several aspects of DV body patterning have already been well documented, and some of the key molecules have been identified. DV patterning of the mesoderm in early embryos leads to tissue-specific differentiation. For example, dorsal explants from early frog embryos differentiate into muscle, and ventral explants form blood (8). In the embryo, mesoderm becomes regionalized to give somites, intermediate mesoderm, and lateral plate mesoderm, going from dorsal to ventral (9). DV body patterning is also crucial for positioning the limbs at the sides of the body. This positioning is accomplished by formation of the apical ectodermal ridge, the thickened epithelium required for limb bud outgrowth, at a DV compartment boundary in the body ectoderm (10). Yet another striking outcome of DV patterning is the difference between back and belly skin or coat color (11). Bmp signaling has been implicated in several of these examples. Thus, graded Bmp signaling specifies mesoderm pattern in early *Xenopus* embryos with high levels specifying ventral mesoderm, which differentiates into blood (12). Mesodermal regionalization in chicken embryos is also controlled by Bmp signaling with high levels of *Bmp4* signaling specifying ventral lateral plate mesoderm (9). Finally, in ventral limb ectoderm, Bmp signaling acts upstream of the gene encoding the transcription factor Engrailed, which is required for proper DV patterning of the limb (13).

Several members of the T-box transcription factor family have been implicated in encoding position in embryos, and *Tbx15* has been shown to play a role in DV specification of skin or coat color. In the absence of *Tbx15* there is dorsal displacement of yellow belly hair in agouti black and tan mice (11). Interestingly, another Tbx gene, *Tbx3*, is associated with mammary gland development. Haploinsufficiency of *Tbx3* has been associated with ulnar-mammary syndrome (UMS) in human patients (14). UMS is an inherited disorder characterized by deficiencies in the ulnar ray in the upper limb and hypoplasia of the mammary glands. In $Tbx3^{-/-}$ mouse embryos there is almost complete failure of initiation of mammary gland development (15).

One attractive possibility is that molecular mechanisms similar to those involved in other aspects of DV patterning are used in

Author contributions: K.-W.C. and J.-Y.K. contributed equally to this work; K.-W.C., J.-Y.K., C.T., and H.-S.J. designed research; K.-W.C., J.-Y.K., S.-J.S., and M.C.E. performed research; E.F. contributed new reagents/analytic tools; K.-W.C., J.-Y.K., S.-J.S., M.C.E., H.-J.K., C.T., and H.-S.J. analyzed data; and K.-W.C., J.-Y.K., C.T., and H.-S.J. wrote the paper.

The authors declare no conflict of interest.

This article is a PNAS direct submission.

Abbreviations: DV, dorsoventral; DiI, 1,19-dioctadecyl-3,3,39,39-tetramethyl indocarbocyanine perchloride; UMS, ulnar-mammary syndrome; E*n*, embryonic day *n*.

¶To whom correspondence should be addressed at: Division in Anatomy and Developmental Biology, Department of Oral Biology, College of Dentistry, Yonsei University, 134 Shinchon-Dong, Seodaemoon-Gu, Seoul 120-752, Korea. E-mail: hsjung@yumc.yonsei.ac.kr.

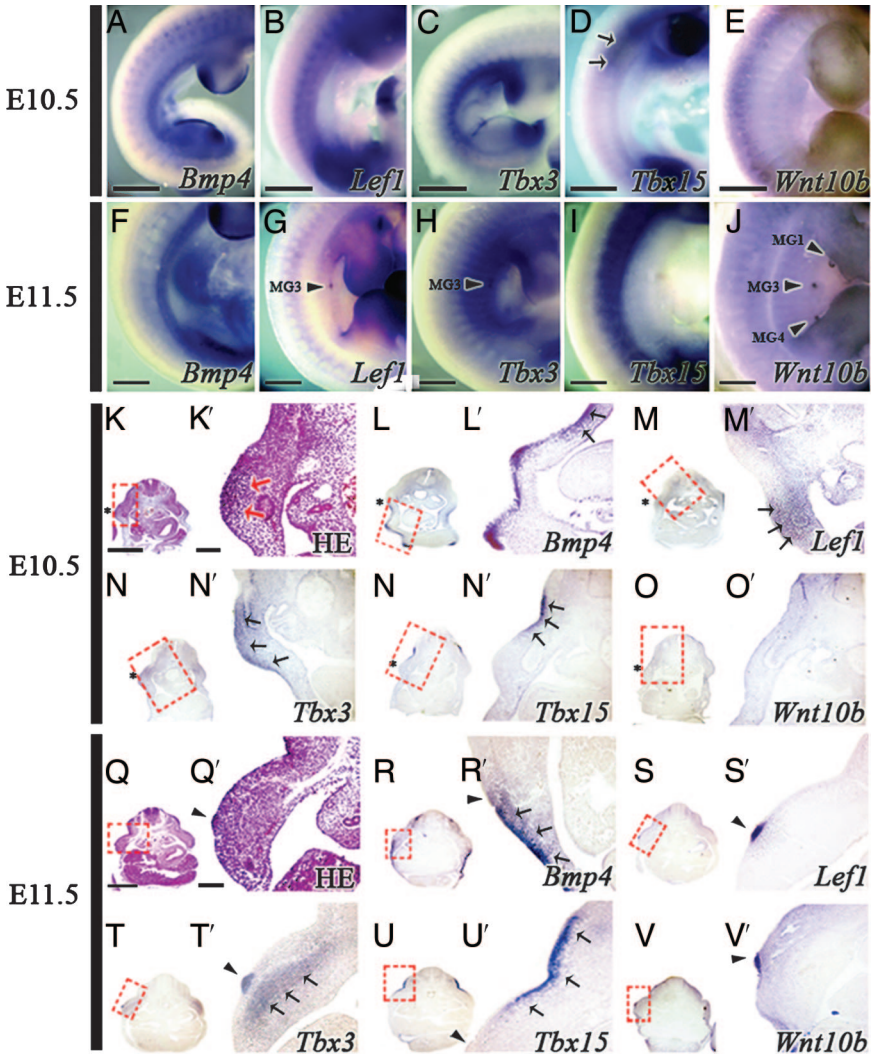

Fig. 1. Gene expression patterns of *Lef1*, *Bmp4*, *Tbx3*, *Tbx15*, and *Wnt10b* in the flank around the time of mammary gland initiation at E10.5 and E11.5. (*A–J*) Whole-mount *in situ* hybridization. (*K–V* and *K′–V′*) Section *in situ* hybridization showing the expression of each gene in serial sections of the same embryo. Histological sections of the mammary gland-forming area at E10.5 (*K* and *K′*) and E11.5 (*Q* and *Q′*) mouse embryos are shown. (*A–E*, *K–P*, and *K′–P′*) E10.5. (*A*) *Bmp4* expressed in the ventral flank. (*L* and *L′*) *Bmp4* expression detected in the flank mesenchyme. (*B*) Broad *Lef1* expression seen in the flank. (*M* and *M′*) *Lef1* was also expressed in the ventral and dorsal regions of the flank. (*C*) *Tbx3* was strongly expressed in the anterodorsal region and was expressed in a broad band in the flank. (*N* and *N′*) A *Tbx3* section showing expression in both the epithelium and mesenchyme. (*D*) *Tbx15* expressed in the anterodorsal part of the body. (*O* and *O′*) *Tbx15* expressed in the mesenchyme. (*E*, *P*, and *P′*) *Wnt10b* expression was not detected in the flank. (*F–J*, *Q–V*, and *Q′–V′*) E11.5. (*F*) *Bmp4* was strongly expressed in the ventral region. (*R* and *R′*) *Bmp4* was strongly expressed in both the epithelium and underlying mesenchyme of the ventral flank. (*G*, *S*, and *S′*) Restricted *Lef1* expression was observed in the epithelium of the third mammary bud (arrowheads) at E11.5. (*H*, *T*, and *T′*) *Tbx3* was expressed in the epithelium and mesenchyme underlying the third mammary bud (arrows). (*I*) *Tbx15* expressed in the dorsal band. (*V* and *V′*) *Tbx15* expressed in the dorsal flank beneath the mesenchyme at E11.5. (*J*, *V*, and *V′*) *Wnt10b* was expressed in the epithelium of the mammary buds. Red dotted boxes indicate areas of higher magnification. Black arrowheads indicate mammary glands (MG1, MG3, and MG4). Asterisks indicate epithelial thickening in a region where the third mammary gland (MG3) will form. Red arrows indicate mesenchymal condensation. Black arrows indicate strong mRNA expressions. (Scale bars: 125 μm.)

formation of the mammary glands. Therefore, we first compared expression patterns of *Bmp4* and *Tbx3* with respect to the DV boundary of the body where mammary gland development is initiated and then tested their involvement in mammary gland positioning. The results have implications for understanding how UMS arises during embryonic development and for the hypothesis that *Bmp* signaling and *Tbx* gene transcription factors are fundamental to DV patterning of the body.

Results

Gene Expression in Relation to the DV Position of Mammary Gland Development. In mice, five individual mammary glands (numbered 1–5 from anterior to posterior) form along two mammary lines running down each side of the ventral region of the body. In embryonic day 10.5 (E10.5) embryos, an epithelial thickening forms in the flank between the forelimb bud and the posterior hindlimb bud (Fig. 1 *K* and *K′*). At E11.5 the third mammary placode is first detected as epithelial thickening (Fig. 1 *Q* and *Q′*), and over the next day the remaining four mammary placodes form. These epithelial thickenings then grow down into the underlying mesenchyme to form bud-like structures (6, 16).

Bmp4, *Lef1*, *Tbx3*, *Tbx15*, and *Wnt10b* gene expression patterns were documented with respect to mammary gland development and the DV boundary in E10.5 and E11.5 mouse embryos using whole-mount *in situ* hybridization (Fig. 1 *A–J*). To determine the precise boundaries of expression of individual genes and to compare precisely expression patterns of different genes, section *in situ* hybridization methods were used and adjacent serial

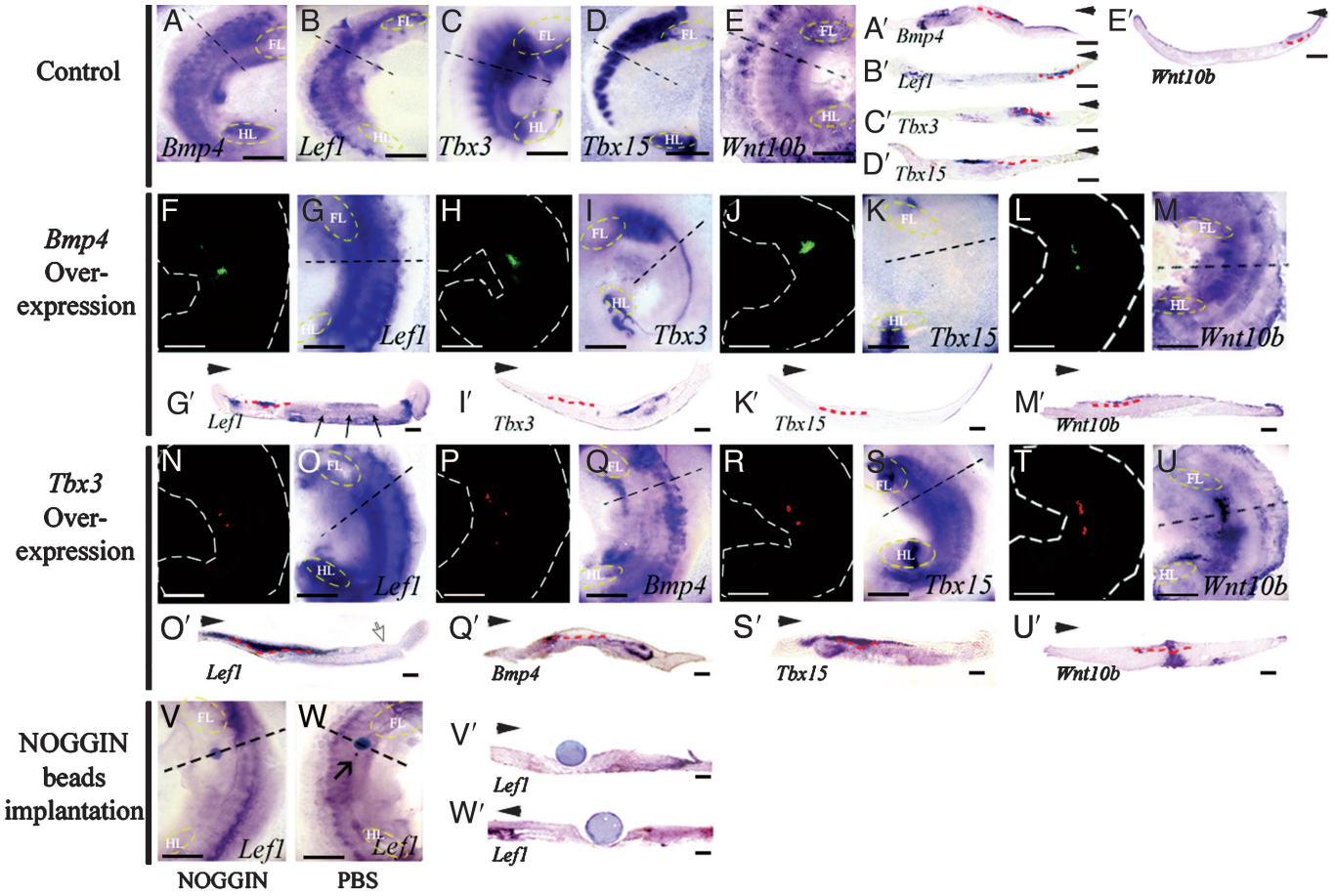

Fig. 2. Mammary gland initiation after manipulation of *Bmp4* signaling and *Tbx3*. (*A–E*) Whole mount *in situ* hybridization after electroporation of E10.0 mouse embryo with a vector containing only fluorescent protein into the right flank. (*F–U*) Overexpression of *Bmp4*–pEGFP-N1 and *Tbx3*–pIRES-DsRed in the ventral flank posterior to the regions of the forelimb bud. The left flank of each E10.0 embryo was used as the experimental side, and the right flank was used as the control. (*A–U*) *In vitro* organ culture for 48 h and whole-mount *in situ* hybridization after electroporation. (*A′–U′*) Transverse sections after *in situ* hybridization of *in vitro* organ cultured tissue. (*F–U*) Dark-field views of ectopic GFP expression (*F–M*) and of DsRed (*N–U*). (*F–M* and *F′–M′*) Overexpression of *Bmp4*. (*G* and *G′*) *Lef1* expression in the dorsal mesenchyme induced by *Bmp4* overexpression in the flank. (*I*, *I′*, *K*, and *K′*) Expression of *Tbx3* and *Tbx15* was reduced by *Bmp4* overexpression. (*M* and *M′*) *Wnt10b* expression; no change after *Bmp4* overexpression. (*N–U* and *N′–U′*) *Tbx3* overexpression. (*O* and *O′*) *Lef1* expression was increased and was more widely expressed, and the epithelium was thickened. (*Q* and *Q′*) *Bmp4* expression was reduced by *Tbx3* overexpression. (*S* and *S′*) *Tbx15* expression extended more ventrally in the flank when *Tbx3* was overexpressed. (*M*, *M′*, *U*, and *U′*) *Wnt10b* was expressed throughout the whole depth of the mesenchyme in the mammary gland-forming area after *Tbx3* overexpression. (*V*, *V′*, *W*, and *W′*) Effect of NOGGIN on gene expression in the developing flank at E10.0. (*V* and *W*) *In vitro* organ cultures 48 h after implanting NOGGIN (*V*) and PBS-soaked beads (*W*) to the flank posterior to the forelimb in E10.0 embryos after whole-mount *in situ* hybridization for *Lef1*. (*V′* and *W′*) Section through beads. (*V* and *V′*) *Lef1* was inhibited in the region around the NOGGIN bead and in the third mammary bud. (*W* and *W′*) No changes in the *Lef1* expression pattern in the flank or third mammary bud were observed (arrow). The yellow dotted line indicates the limb. FL, forelimb; HL, hindlimb. The red dotted line indicates the basement membrane of epithelial thickening. The black dotted line indicates the section level. The white dotted line indicates the outlining of embryo. The point of each arrowhead indicates dorsal direction. The open arrows indicate the ventral margin of the somite region. The filled arrows in *G′* indicate the mesenchymal *Lef1* ectopic expression after *Bmp4* overexpression. (Scale bars: 150 μm.)

sections were examined (Fig. 1 *L–P*, *L′–V′*, *R–V*, and *R′–V′*). At E10.5 *Lef1* was detected in both ventral and dorsal regions of the flank (Fig. 1 *B*, *M*, and *M′*) whereas *Bmp4* expression in the ectoderm and underlying mesenchyme was observed ventrally (Fig. 1 *A*, *L*, and *L′*). *Tbx3* was expressed in a broad band all along the anteroposterior axis of the flank between forelimb and hindlimb (Fig. 1*C*), with strong expression in the thickened epithelium that forms the mammary line and underlying mesenchyme (Fig. 1 *N* and *N′*). *Tbx15* was expressed in the dorsal region of the flank between forelimb and hindlimb in epithelium and underlying mesenchyme (Fig. 1 *D*, *O*, and *O′*). *Wnt10b* was not detected in the flank region of the E10.5 embryos (Fig. 1 *E*, *P*, and *P′*). At E11.5 *Lef1* was expressed in the discrete epithelial thickening, which is the earliest sign of the third mammary bud (Fig. 1 *G*, *S*, and *S′*) whereas *Bmp4* was still expressed in both ventral epithelium and underlying mesenchyme (Fig. 1*F*). Compared with E10.5, *Bmp4* expression was much stronger in the epithelium and weaker in the mesenchyme (Fig. 1 *R* and *R′*). At E11.5 the intensity of *Tbx3* expression was much higher than E10.5 (Fig. 1*H*). Section *in situ* hybridization showed that *Tbx3* is expressed in both epithelium and mesenchyme in the area in which the third mammary bud is forming (Fig. 1 *T* and *T′*) whereas *Tbx15* expression was dorsal and restricted to mesenchyme just beneath epithelium (Fig. 1 *I*, *U*, and *U′*). At E11.5 *Wnt10b* expression was observed not only in the third mammary gland (MG3) but also in the first (MG1) and fourth (MG4) mammary glands (Fig. 1 *J*, *V*, and *V′*).

***Bmp4* and *Tbx3* Play Key Roles in DV Patterning of Mammary Glands.** To test the interactions between *Bmp4* and *Tbx3* we electroporated expression constructs containing either *Bmp4* or *Tbx3* together with a fluorescent reporter protein into the mouse flank

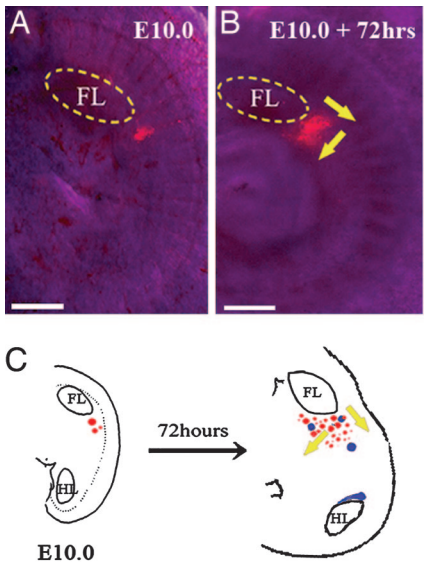

Fig. 3. Tracing cell movement by DiI microinjection. (*A*) DiI injected into the ventral–lateral flank posterior to the forelimb bud of E10.0. (*B*) After culturing the flank for 72 h in *in vitro* organ culture DiI labeling was monitored to trace the fate of marked cells. (*C*) Schematic diagrams showing experiments and results together with the location of the mammary glands. FL, forelimb; HL, hindlimb. Red spots, DiI; blue spots, mammary buds; yellow arrows, displacement of DiI-labeled cells. (Scale bars: 125 μm.)

posterior to the forelimb at E10.0, and the electroporated mouse flank was then placed in *in vitro* organ culture for 48 h. Expression patterns of *Lef1*, *Bmp4*, *Tbx3*, *Tbx15*, and *Wnt10b* were then examined to elucidate the signaling network that specifies the formation of mammary glands. Fig. 2 *A–E* and *A′–E′* shows expression of these genes in controls in which only the vector expressing fluorescent protein was electroporated.

After overexpression of both *Bmp4* (Fig. 2 *F*, *H*, *J*, and *L*) and *Tbx3* (Fig. 2 *N*, *P*, *R*, and *T*), *Lef1* expression increased in the flank (Fig. 2 *G* and *O*). Transverse sections showed that, after *Tbx3* overexpression in the flank, the thickened epithelium expressing *Lef1* was dorsally extended toward the somite-forming region and dorsal midline ($n = 26/30$; 86.7%) (Fig. 2*O′*) rather than being a discrete epithelial thickening expressing *Lef1* as in the control third mammary bud. In four cases the thickened epithelium appeared to be extended bidirectionally. The sections also confirmed that the intensity of *Lef1* expression was more pronounced than in controls (compare Fig. 2 *B′*, *G′*, and *O′*). In contrast, *Bmp4* overexpression did not alter the morphogenesis of the mammary gland-forming epithelium, and only the discrete thickening associated with the third mammary bud was present ($n = 30/30$; 100%) (Fig. 2*G′*).

To examine further the regulation of *Lef1* by *Bmp4*, beads soaked in the Bmp antagonist NOGGIN were implanted posterior to the forelimb in E10.0 mouse embryo flank and then cultured for 48 h. This application of NOGGIN resulted in local inhibition of *Lef1* expression ($n = 30$; frequency of inhibition 70%) (Fig. 2 *V* and *V′*). As controls, beads soaked in PBS were implanted ($n = 30$), and in these cultures *Lef1* expression was unaffected (Fig. 2 *W* and *W′*). These data confirm that Bmps regulate *Lef1* expression. Thus both *Tbx3* and *Bmp4* appear to play key roles in mammary gland initiation by regulating *Lef1* expression.

Lef1 and *Wnt10b* expression patterns were similar in early mammary gland development, with the genes being expressed in a raised streak of lateral body wall epithelium at E11.5 (Fig. 1 *G*, *J*, *S*, *S′*, *V*, and *V′*). However, after *Tbx3* and *Bmp4* overexpression, expression of *Wnt10b* did not respond in the same way as expression of *Lef1*. Thus, *Wnt10b* expression was not changed by *Bmp4* overexpression ($n = 26/30$; 86.7%) (Fig. 2 *M* and *M′*)

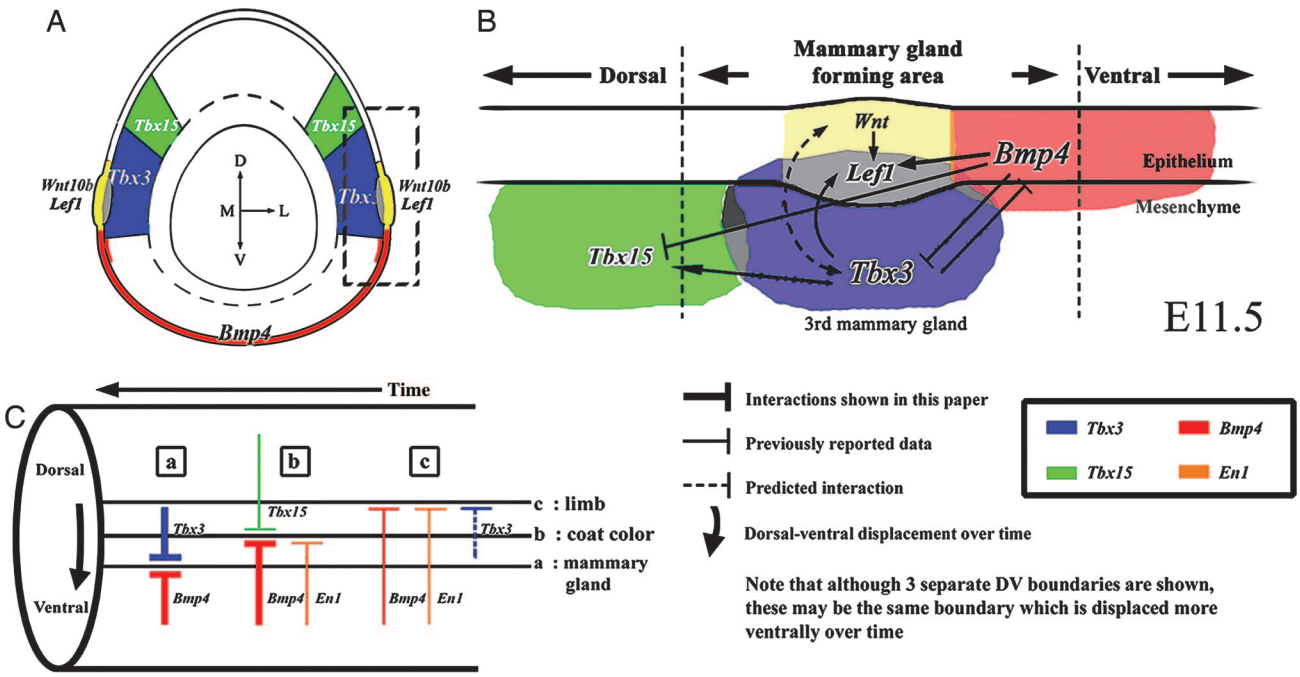

Fig. 4. Schematic diagrams showing position-dependent patterns of gene expression along the DV body axis (*A*), interactions controlling the position of mammary gland development at E11.5 (*B*), and a comparison of DV patterning with respect to the mammary glands, coat color, and limbs (*C*). (*A*) Transverse section showing patterns of gene expression in relation to the DV axis. (*B*) Regulatory gene interactions that establish DV patterns of gene expression at E11.5 in the mammary gland-forming region and govern the position of mammary gland initiation. Note that it was not elucidated whether these interactions are direct or indirect. (*C*) Lateral view of the flank showing interactions. (*a*) Positioning the mammary glands. (*b*) Determining coat color boundary. (*c*) Positioning the limbs. Note that although three separate DV boundaries are shown, these may be the same boundary that is displaced ventrally over time. D, dorsal; V, ventral; M, medial; L, lateral.

whereas, in contrast, after *Tbx3* overexpression *Wnt10b* was expressed not only in the epithelium but also in the whole depth of mesenchyme under the third mammary gland-forming area ($n = 29/30$; 96.6%) (Fig. 2 *E*, *E′*, *U*, and *U′*).

Bmp4 overexpression led to changes in *Tbx3* and *Tbx15* expression patterns (Fig. 2 *I*, *I′*, *K*, and *K′*). Overexpression of *Bmp4* completely abolished *Tbx15* expression in the flank region ($n = 30/30$; 100%) (Fig. 2 *K* and *K′*), and *Tbx3* expression was almost completely inhibited except in the mesenchyme along the DV border between the somite-forming area and dorsal flank ($n = 29/30$; 96.6%) (Fig. 2 *I* and *I′*). These results suggest that *Bmp4* signaling regulates the extent of expression of *T-box* genes along the DV axis of the flank.

There were also changes in *Tbx15* and *Bmp4* expression after *Tbx3* overexpression ($n = 30/30$; 100%) (Fig. 2 *Q*, *Q′*, *S*, and *S′*). *Tbx15* expression was expanded into both dorsal and ventral mesenchyme at the site of the epithelial thickening that marked the mammary line (compare Fig. 2 *D*, *D′*, *S*, and *S′*). *Bmp4* expression, in contrast, was inhibited where *Tbx3* was overexpressed in the flank region ($n = 30/30$; 100%) (compare Fig. 2 *A*, *A′*, *Q*, and *Q′*).

So what is the relationship between the DV boundary at which the limbs develop and that at which mammary glands form? To address this question, we used the lipophilic dye 1,19-dioctadecyl-3,3,39,39-tetramethyl indocarbocyanine perchloride (DiI) to follow cell fate during early mammary gland formation (Fig. 3). We labeled cells with DiI in the flank just posterior to the limb bud at the same DV level as the limb bud. After 72 h of culture the patch of DiI-labeled cells had extended not only posteriorly along the flank but also more ventrally to occupy the area of the forming mammary glands (Fig. 3).

Discussion

From our results we propose a model for DV patterning of mammary glands. We have shown that expression domains of *Bmp4*, *Lef1*, *Tbx3*, *Tbx15*, and *Wnt10b* are specifically localized to different DV levels around the body at the time when mammary gland development is initiated at E11.5 (Fig. 4*A*). *Tbx3* is expressed in the epithelium of the mammary bud and the mesenchyme underlying *Lef1* and *Wnt10b* expression, which marks the DV position at which mammary glands develop, whereas *Tbx15* and *Bmp4* are expressed dorsally and ventrally, respectively. These striking position-dependent patterns of gene expression along the DV body axis just before and during early mammary gland formation suggest that interactions between these genes, in particular *Bmp4* and *Tbx3*, might control body patterning with respect to mammary gland formation.

We tested this hypothesis by overexpressing *Bmp4* and *Tbx3* in cultured mouse flanks. Our overexpression experiments showed that there is reciprocal negative regulation between *Bmp4* and *Tbx3* (Fig. 4*B*) and that overexpression of *Tbx3* could induce *Lef1* expression and produce a DV extension of the epithelial thickening of the ectoderm characteristic of the mammary placode. Thus, we propose that inhibitory effects of *Bmp4* on *Tbx3* might establish a DV boundary, which would then serve to confine *Lef1* expression and thickened mammary epithelium to a particular position with respect to the DV body axis. Our experiments with NOGGIN suggest that Bmp signaling also plays a role in maintaining *Lef1* expression in the mammary placode.

How does *Tbx3* induce *Lef1* expression and a thickened mammary placode? As in tooth development (17), *Lef1* might direct mesenchymal condensation and be involved in the Wnt pathway that induces an epithelial thickening. *Wnt10b* and *Wnt6* are expressed along the DV boundary of the flank and then become confined to the mammary placodes (16, 18). Consistent with a role for *Wnt10b*, we found that, when *Tbx3* was overexpressed, *Wnt10b* expression was increased in the mesenchyme of the mammary ridge. Thus, *Tbx3* may play a crucial role at the DV boundary by controlling *Wnt10b* and *Lef1* expression and mammary gland initiation (Fig. 4*B*). These data are consistent with observations on $Tbx3^{-/-}$ mouse embryos, in which neither *Lef1* nor *Wnt10b* could be detected in the regions where mammary glands normally form (15, 16). The proposed involvement of *Tbx3* in both setting a DV boundary of the body and initiating mammary gland development could explain why mammary glands fail to form in $Tbx3^{-/-}$ embryos and why, in UMS, which is caused by *Tbx3* haploinsufficiency, mammary glands are reduced.

There are striking similarities between the mechanisms that we propose for mammary gland positioning and those that control DV coat color and position the limbs (Fig. 4*C*). We have proposed that antagonistic interactions between *Bmp4* and *Tbx3* are involved in initiation of mammary gland formation at a particular DV level (Fig. 4*C*). From this viewpoint, observations on UMS human patients (19) together with absence of mammary glands in $Tbx3^{-/-}$ mouse embryos might be considered in terms of ventralization of the flank. We have also shown that *Bmp4* signaling inhibits expression of *Tbx15*, which has previously been shown to specify dorsal coat color and have a complementary expression pattern to *En1* (Fig. 4*C*) (11). Work by others has shown that, in the absence of *Tbx15*, the belly coat color extends more dorsally and therefore again could be considered to be due to (partial) ventralization of the flank (11). Finally, previous work has shown that Bmp4 signaling upstream of *En1* also specifies the ventral ectodermal compartment and controls ventral limb pattern (13). Limb bud development occurs much earlier than mammary gland development, and, because fingers can be dorsalized in some human patients with UMS (14, 19), we suggest that, at this earlier stage, *Tbx3* may act in concert with *Bmp4* to specify ventral limb pattern. Indeed, the importance of Bmp signaling in maintaining *Tbx3* expression in the developing limb is well documented (20).

It is not clear whether the same DV boundary operates in all three patterning processes. We have shown that cells that participate in mammary gland formation originate more dorsally and then become displaced ventrally. Furthermore, *Tbx15* expression has been reported to extend more ventrally as development proceeds. Therefore, it is possible that the same boundary is used but by means of different target genes, including two gene members of the *Tbx* family, and at successive times in development.

Materials and Methods

All experiments were performed according to the guidelines of the Intramural Animal Use and Care Committee of Yonsei University College of Dentistry.

Animals. Adult Institute of Cancer Research mice were housed in a temperature-controlled room (22°C) under artificial illumination (lights on from 0500 to 1700 hours) and 55% relative humidity. The mice had access to food and water ad libitum. Embryos were obtained from time-mated pregnant mice. E0 was designated as the day a vaginal plug was confirmed. Embryos at developmental stages E10.0, E10.5, and E11.5 were used in this study.

***in Vitro* Organ Culture.** Institute of Cancer Research mouse embryos were isolated at E10.0 and placed in culture medium (BGJb; Sigma, St. Louis, MO) augmented with 0.5% penicillin/streptomycin and 0.2% ascorbic acid as previously described (6). Briefly, individual embryos were dissected into left and right halves by using fine tungsten needles to bisect the neural tube. The left flank was the experimental tissue, and the right acted as control. Each flank tissue was placed on filter membranes (Track-etch, 1.0-μm pore; Whatman Nuclepore), which were supported on stainless steel grids in sterile culture dishes, and cultured at the air–medium interface at 37°C and 7.5% CO_2 for 48 and 72 h. Culture medium was replaced at 24 h. Tissues were

then fixed and processed for *in situ* hybridization. At least 30 explants were used in each experiment.

DiI Microinjection. DiI (Molecular Probes, Eugene, OR) is a vital, highly fluorescent, lipophilic dye belonging to the carbocyanine dye family. After DiI microinjection into designated regions of the flank, the migration pattern of DiI-labeled cells was observed at 72 h by using fluorescence microscopy (MZ-FLIII; LEICA, Jena, Germany).

***In Situ* Hybridization.** *In situ* hybridization was performed as previously described by Kim *et al*. (21). Section *in situ* hybridization was performed as previously described on wax sections by using standard protocols (21). Briefly, embryos were fixed in 4% paraformaldehyde, embedded in paraffin wax, and sectioned at 12 μm. The following DNA plasmids were used as templates for the synthesis of digoxigenin-labeled RNA probes: *Bmp4* and *Lef1* (from Yi-Ping Chen, Tulane University, New Orleans, LA); *Tbx3* and *Tbx15* (from Gregory S. Barsh, Stanford University School of Medicine, Stanford, CA); and *Wnt10b*.

Bead Implantation. Affigel Blue beads (Bio-Rad), 150 μm in diameter, were washed with PBS and then soaked in 0.5 mg/ml human recombinant NOGGIN (Regeneron). Beads were implanted in the flank region along the mammary line of E10.0 mouse embryos.

Expression Constructs. Constructs were pEGFP-N1 and pIRES-DsRed, both of which have been optimized for generating proteins with brighter fluorescence (Clontech). *Bmp4* was inserted into the blunted EcoRI/HindIII sites of pEGFP-N1, and *Tbx3* was inserted into the XhoI/BamHI sites of pIRES-DsRed.

Electroporation. Plasmid DNA was purified by using a plasmid purification kit (Qiagen, Valencia, CA) and dissolved in T1/4E (10 mM Tris·HCl, pH 8.0/0.25 mM EDTA). Fast Green at 1/10,000 (Sigma) was added to the DNA solution for visualization within the tissue. A microcapillary needle was used to inject $\approx$1 μg/μl DNA into the flank mesenchyme, after which 20-ms current pulses of 25 V were applied with an electroporator. The experimental group comprised the left flank electroporated with either *Bmp4* in pEGFP-N1 or *Tbx3* in pIRES-DsRed construct. The right flank was electroporated with constructs containing only fluorescent proteins (EGFP and DsRed) and used as controls.

We thank Dr. Christine Campbell (State University of New York, Buffalo, NY) for the *Tbx3* full-length cDNA. This research was supported by Grant R13-2003-13 from the Basic Research Program of the Korea Science and Engineering Foundation and a Royal Society Korea–U.K. joint project grant (to H.-S.J. and C.T.). C.T. receives additional support from The Royal Society. M.C.E. was supported by an Anatomical Society Research Scholarship.

1. Wolpert L (2003) *Development (Cambridge, UK)* 130:4497–4500.
2. Veltmaat JM, Relaix F, Le LT, Kratochwil K, Sala FG, van Veelen W, Rice R, Spencer-Dene B, Mailleux AA, Rice DP, *et al.* (2006) *Development (Cambridge, UK)* 133:2325–2335.
3. Merkel F (1901) in *Henle's Grundriss der Anatomiedes des Menschen, Atlas*, (Friendrich Vieweg und Sohn, Braunschweig, Germany), 4th Ed, p 247.
4. Kollmann J (1907) in *Handatlas der Entwicklungsgeschichte des Menschen*, Zweiter Teil. Integmentum commune et Organa sensuum (Gustav Fischer, Jena, Germany), Fig 654.
5. van Genderen C, Okamura RM, Farinas I, Quo RG, Parslow TG, Bruhn L, Grosschedl R (1994) *Genes Dev* 8:2691–2703.
6. Eblaghie MC, Song S-J, Kim J-Y, Akita K, Tickle C, Jung H-S (2004) *J Anat* 205:1–13.
7. Veltmaat JM, Mailleux AA, Thiery JP, Bellusci S (2003) *Differentiation* 71:1–17.
8. Jones CM, Dale L, Hogan BL, Wright CV, Smith JC (1996) *Development (Cambridge, UK)* 122:1545–1554.
9. Tonegawa A, Funayama N, Ueno N, Takahashi Y (1997) *Development (Cambridge, UK)* 124:1975–1984.
10. Altabef M, Clarke JD, Tickle C (1997) *Development (Cambridge, UK)* 124: 4547–4556.
11. Candille SI, Van Raamsdonk CD, Chen C, Kuijper S, Chen-Tsai Y, Russ A, Meijlink F, Barsh GS (2004) *PLoS Biol* 2:30–42.
12. Dosch R, Gawantka V, Delius H, Blumenstock C, Niehrs C (1997) *Development (Cambridge, UK)* 124:2325–2334.
13. Pizette S, Abate-Shen C, Niswander L (2001) *Development (Cambridge, UK)* 128:4463–4474.
14. Bamshad M, Le T, Watkins WS, Dixon ME, Kramer BE, Roeder AD, Carey JC, Root S, Schinzel A, Van Maldergem L, *et al.* (1999) *Am J Hum Genet* 64:1550–1562.
15. Davenport TG, Jerome-Majewska LA, Papaioannou VE (2003) *Development (Cambridge, UK)* 130:2263–2273.
16. Veltmaat JM, Van Veelen W, Thiery JP, Bellusci S (2004) *Dev Dyn* 229:349–356.
17. Sasaki T, Ito Y, Xu X, Han J, Bringas P, Jr, Maeda T, Slavkin HC, Grosschedl R, Chai Y (2005) *Dev Biol* 278:130–143.
18. Lane TF, Leder P (1997) *Oncogene* 15:2133–2144.
19. Sasaki G, Ogata T, Ishii T, Hasegawa T, Sato S, Matsuo N (2002) *Am J Med Genet* 110:365–369.
20. Tumpel S, Sanz-Ezquerro JJ, Isaac A, Eblaghie MC, Dobson J, Tickle C (2002) *Dev Biol* 250:251–262.
21. Kim J-Y, Cho SW, Lee MJ, Hwang HJ, Lee JM, Lee SI, Muramatsu T, Shimono M, Jung H-S (2005) *Cell Tissue Res* 320:409–415.